Accepted Manuscript

Phthalocyanine–sulfonamide conjugates: Synthesis and photodynamic inactivation of Gram-negative and Gram-positive bacteria

Raquel Nunes da Silva, Ângela Cunha, Augusto C. Tomé

PII: S0223-5234(18)30413-6

DOI: 10.1016/j.ejmech.2018.05.009

Reference: EJMECH 10419

To appear in: *European Journal of Medicinal Chemistry*

Received Date: 14 March 2018

Revised Date: 11 April 2018

Accepted Date: 7 May 2018

Please cite this article as: R.N. da Silva, Â. Cunha, A.C. Tomé, Phthalocyanine–sulfonamide conjugates: Synthesis and photodynamic inactivation of Gram-negative and Gram-positive bacteria, *European Journal of Medicinal Chemistry* (2018), doi: 10.1016/j.ejmech.2018.05.009.

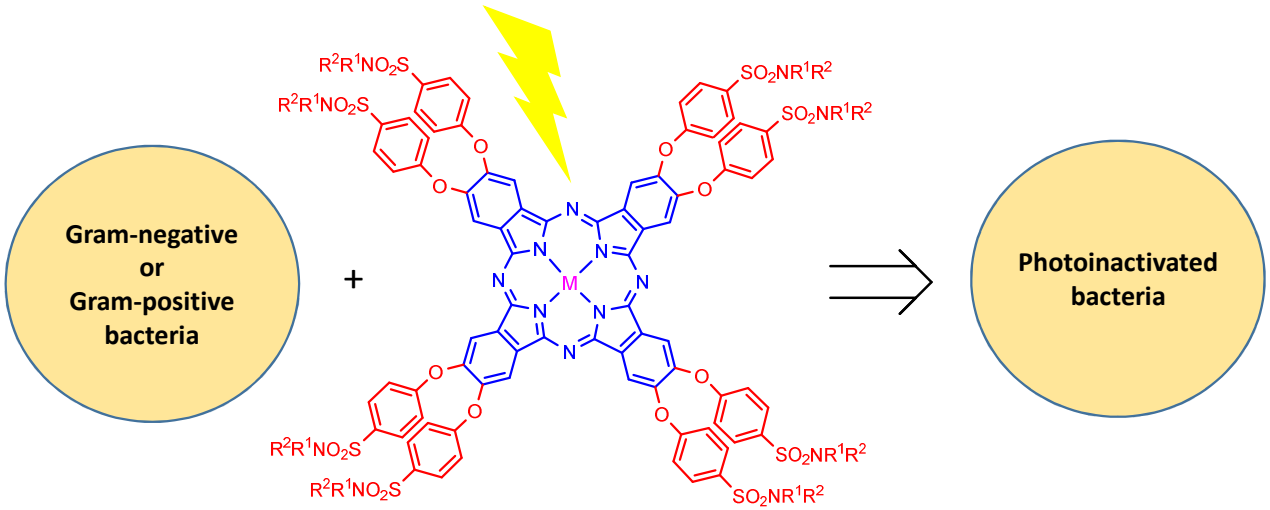
Gram-negative
or
Gram-positive
bacteria
+
M
Photoinactivated
bacteria

Phthalocyanine–sulfonamide conjugates: synthesis and photodynamic inactivation of Gram-negative and Gram-positive bacteria

Raquel Nunes da Silva,[a, b] Ângela Cunha[*b] and Augusto C. Tomé[*a]

[a]*Department of Chemistry & QOPNA, University of Aveiro, 3810-193 Aveiro, Portugal*

[b]*Department of Biology & CESAM, University of Aveiro, 3810-193 Aveiro, Portugal*

*actome@ua.pt, acunha@ua.pt

Corresponding Author:

Augusto C. Tomé

Email: actome@ua.pt

Address: Department of Chemistry & QOPNA, University of Aveiro, 3810-193 Aveiro, Portugal

Declarations of interest: none.

Abstract: Phthalocyanines bearing four or eight sulfonamide units were synthesized and their efficiency in the photodynamic inactivation of Gram-negative (*Escherichia coli*) and Gram-positive (*Staphylococcus aureus*) bacteria was evaluated. Conjugates with simpler sulfonamide units (*N*,*N*-diethylbenzenesulfonamide, *N*-isopropylbenzenesulfonamide and *N*-(4-methoxyphenyl)benzenesulfonamide) caused stronger inactivation than those with heterocyclic groups (*N*-(thiazol-2-yl)benzenesulfonamide) or long alkyl chains (*N*-dodecylbenzenesulfonamide) in both bacteria. Furthermore, the encapsulation of the phthalocyanine–sulfonamide conjugates within polyvinylpyrrolidone micelles, used as drug delivery vehicles, in general showed to enhance the inactivation efficiency. The results show that encapsulated phthalocyanine–sulfonamide conjugates are a promising class of photosensitizers to be used in photodynamic antimicrobial therapy.

Keywords: Phthalocyanine, Sulfonamide, Photosensitizer, Photodynamic inactivation, Antimicrobial, *E. coli*, *S. aureus*

1. Introduction

Phthalocyanines (Pcs) are synthetic aromatic macrocycles that, although having a structure similar to that of natural porphyrins, are not found in Nature. Due to their structural and electronic properties, Pcs have been used in a wide range of applications [1,2]. Taking advantage of their absorbance in the red region of the UV–Vis spectrum, typically between 620–700 nm, Pcs have been successfully used or tested as photosensitizers (PSs) in various medical applications [3], mainly for the treatment of cancer by photodynamic therapy (PDT) [4–6], in the photodynamic inactivation of microorganisms (PDI) [7,8], and also as theranostic agents [9–11]. Pcs are also being studied as potential drugs for the treatment of amyloid related neurological disorders [12]. Their use in chemical sensors [13,14], microbial fuel cells [15,16], DNA interaction [17,18], catalysis [19], and in solar cells [20,21] is frequently reported. The functionalization of the periphery of Pcs allows the modulation of their properties and the design of compounds with new potentialities. The insertion of sulfonamide (SA) groups at the periphery of the phthalocyanine (Pc) with the purpose of improving the efficacy and selectivity to particular targets in frontier structures of bacteria is an example of such application-designed modifications.

Sulfonamides are frequently used as antimicrobials [22,23]. Antimicrobial SAs exhibit a broad spectrum of action, covering all organisms that synthesize folic acid *de novo* through the folate pathway (they inhibit the enzyme dihydropteroate synthase (DHPS)) [24]. This biosynthetic pathway is present in many pathogenic microorganisms but, crucially, it is absent in mammals. This makes the folate pathway attractive as an antimicrobial drug target. In recent years, SAs have also been tested as inhibitors or activators of enzymes in various biological systems [25–31].

The conjugation of drugs with phthalocyanines [32] porphyrins [33–35] or other chromophores [36–38] has been reported. An interesting example of such conjugates was recently produced by Jung *et al*. [36] and involved the synthesis of a boron-dipyrromethene (BODIPY) covalently linked to acetazolamide (a SA). That conjugate was designed to take advantage of the acetazolamide properties (to assure both carbonic anhydrase IX inhibition and efficient tumour targeting) combined with the

ability of the BODIPY moiety to generate singlet oxygen and to allow to track the cellular uptake and distribution by fluorescence. *In vitro* studies with Human breast cancer cells (MDA-MB-231 cells), that overexpress carbonic anhydrase IX, revealed accumulation of the conjugate in mitochondria and singlet oxygen generation by irradiation at 660 nm. *In vivo* studies with that conjugate in xenograft mouse models revealed remarkable tumour suppression.

Since Pcs are generally not soluble in water and in most organic solvents, several strategies have been developed to overcome this issue. One of them involves the decoration of the Pc periphery with suitable substituents that can enhance their solubility [39–41]. Alternatively, Pcs can be encapsulated in drug delivery vehicles such as micelles, conjugated polymer nanoparticles or inorganic nanoparticles. In particular, polyvinylpyrrolidone (PVP) micelles have been successfully used as drug vehicles in several studies [42–46].

Considering the potential of Pcs as PSs and SAs as antibacterial molecules, we decided to synthesize Pc–SA conjugates and to use them as PSs in photodynamic antimicrobial therapy, taking advantage of the effects of both components. The Pc–SA conjugates were used in the PDI of a Gram-negative (*Escherichia coli*) and a Gram-positive (*Staphylococcus aureus*) bacteria, either in solution or encapsulated in PVP micelles.

2. Results and discussion

2.1. Synthesis and encapsulation

The synthetic route used to obtain the phthalonitrile derivatives and the corresponding Pcs is summarized in Scheme 1. Compounds **6**, **9** and **10** were prepared as already reported [47,48]; compounds **3**, **7** and **8** were synthesized following a similar procedure. The Pcs were prepared by tetramerization of the corresponding phthalonitriles. The synthesis of phthalocyanines **Zn11**, **Zn14** and **Zn15** has already been reported [47,48].

The encapsulation of phthalocyanines **11**, **12**, **14** and **Zn11**–**Zn16** within the water soluble polyvinylpyrrolidone was performed in an incubator at 50 °C overnight. The Pcs were completely dissolved, yielding blue-green solutions.

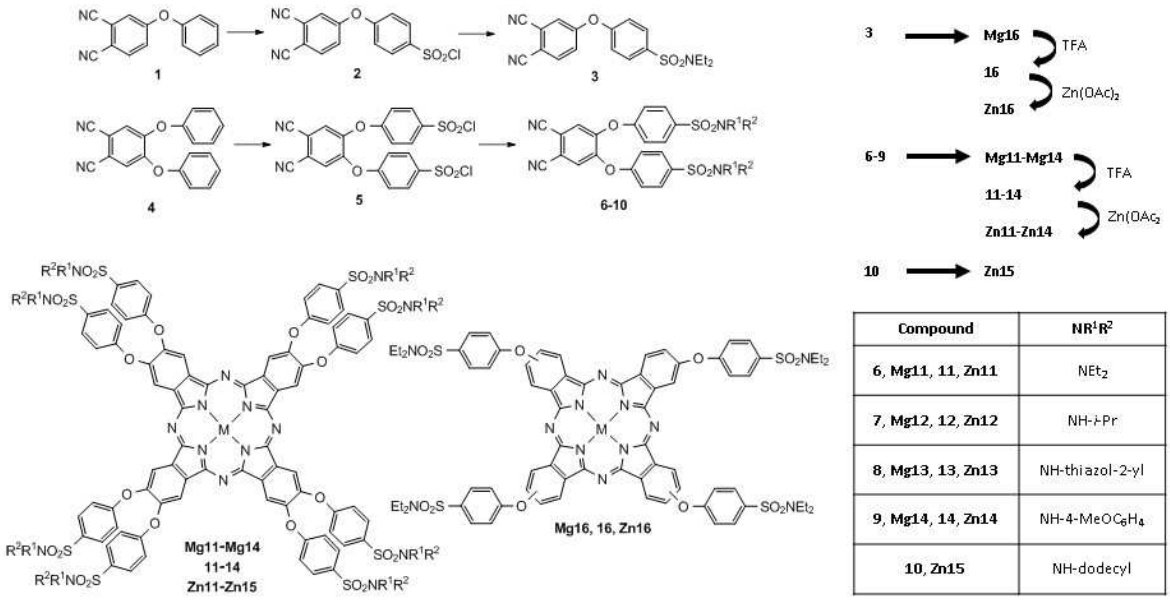

Compound	NR^1R^2
6, Mg11, 11, Zn11	NEt_2
7, Mg12, 12, Zn12	NH-*i*-Pr
8, Mg13, 13, Zn13	NH-thiazol-2-yl
9, Mg14, 14, Zn14	NH-4-$MeOC_6H_4$
10, Zn15	NH-dodecyl

Scheme 1. Synthesis of Pc–SA conjugates.

2.2. Solubility, photosensitizing properties and photostabilities

The solubility of the selected Pcs, in PBS + 10% DMSO, and the corresponding Pc(PVP), in PBS, was analysed by UV–Vis spectroscopy. The measurements were made in concentrations between 2.5 µmol/L and 25 µmol/L in order to determine if the Pcs, at this concentration range, follow the Beer–Lambert law. The graphics were obtained by plotting the Q-band intensity *versus* the Pc concentration in DMSO. A linear relation was observed for all zinc and metal-free Pcs, indicating low aggregation in this solvent at these concentrations. However, in PBS + 10% DMSO the relation was not linear. A similar approach was used to evaluate the solubility of Pcs encapsulated within PVP in PBS. A linear relation was observed for all Pc(PVP) (Fig. S6–S14).

The results of the evaluation of the singlet oxygen generation by each PS, measured as the photo-oxidation of DPBF when irradiated at an irradiance of 9.0 mW/cm^2, showed that in DMF all Pcs were excellent singlet oxygen generators (Table 1) but in the aqueous medium (PBS + 10% DMSO) there was a negligible photo-degradation of the DPBF for all Pcs under study. However, a 59–91% photo-degradation of the DPBF was observed for the Pc(PVP) conjugates in PBS (Table 1).

The encapsulation of the synthesized Pcs in PVP, intended to improve their solubility in aqueous media, was successful and, in addition, singlet oxygen generation in aqueous

media was also enhanced with Pc(PVP) photosensitizers. This can be related with the accommodation of the Pcs within micelles in the monomeric state. A similar strategy was used by Lian *et al.* [43] that reported the preparation of a multifunctional delivery vehicle involving a PS (a zinc Pc) and a targeting agent (folic acid) encapsulated within PVP micelles that was used as a PS in *in vitro* and *in vivo* studies. In addition, the interaction of PVP with chlorin e6 derivatives bearing one α-amino acid or 6-aminohexanoic acid as substituent was also demonstrated, confirming PVP as an useful drug carrier in PDT and consequently in PDI [42]. Singlet oxygen generation by Pc(PVP) in aqueous medium was interestingly high, with percentages of DPBF oxidation similar to the ones obtained for the Pcs in DMF. These differences may even be somewhat underestimated because of the presence of DMSO, a well-known $^1O_2$ quencher [49]. Also, the lower singlet oxygen generation observed for Pc(PVP) in PBS, when compared with DMF suspensions, seems to indicate that some aggregation is still occurring. In general, the results demonstrate that PVP encapsulation represents an improvement in the photosensitization process, in particular when Pcs with low solubility in aqueous media are used. The encapsulation procedure is simple enough to be performed overnight, making PVP more practical and cost-effective than other drug delivery vehicles like silica or gold nanoparticles.

The results of the photostability studies conducted during 30 min with red light, with an irradiance of 150 mW/cm^2, showed that all Pcs are photostable.

Table 1 Relative photo-oxidation of DPBF by singlet oxygen generated by Pcs in DMF and PBS + 10% DMSO and Pc(PVP) in PBS. [a] After 7 minutes of irradiation. DMSO used in the second column was maintained in less than 10% final concentration. [b] Results obtained with Pc(PVP) conjugates.

Compound	DPBF decay (%)[a]		
	DMF	PBS + DMSO	PBS[b]
11	93	1	68
12	96	4	74
14	92	4	59
Zn11	95	5	79
Zn12	100	1	80
Zn13	99	5	85

Zn14	99	5	78
Zn15	99	5	91
Zn16	94	6	71

2.3. Relation between bioluminescence and concentration of viable cells

A significant linear correlation between bioluminescence and viable counts for the bioluminescent *E. coli* strain was observed (R^2 = 0.9526) (Fig. S15).

2.4. Photodynamic inactivation of E. coli and S. aureus

The log reductions obtained in the PDI assays with *E. coli* and *S. aureus* are summarized in Fig. 1 and detailed in the SI (Fig. S16–S21 and Fig. S22–S25).

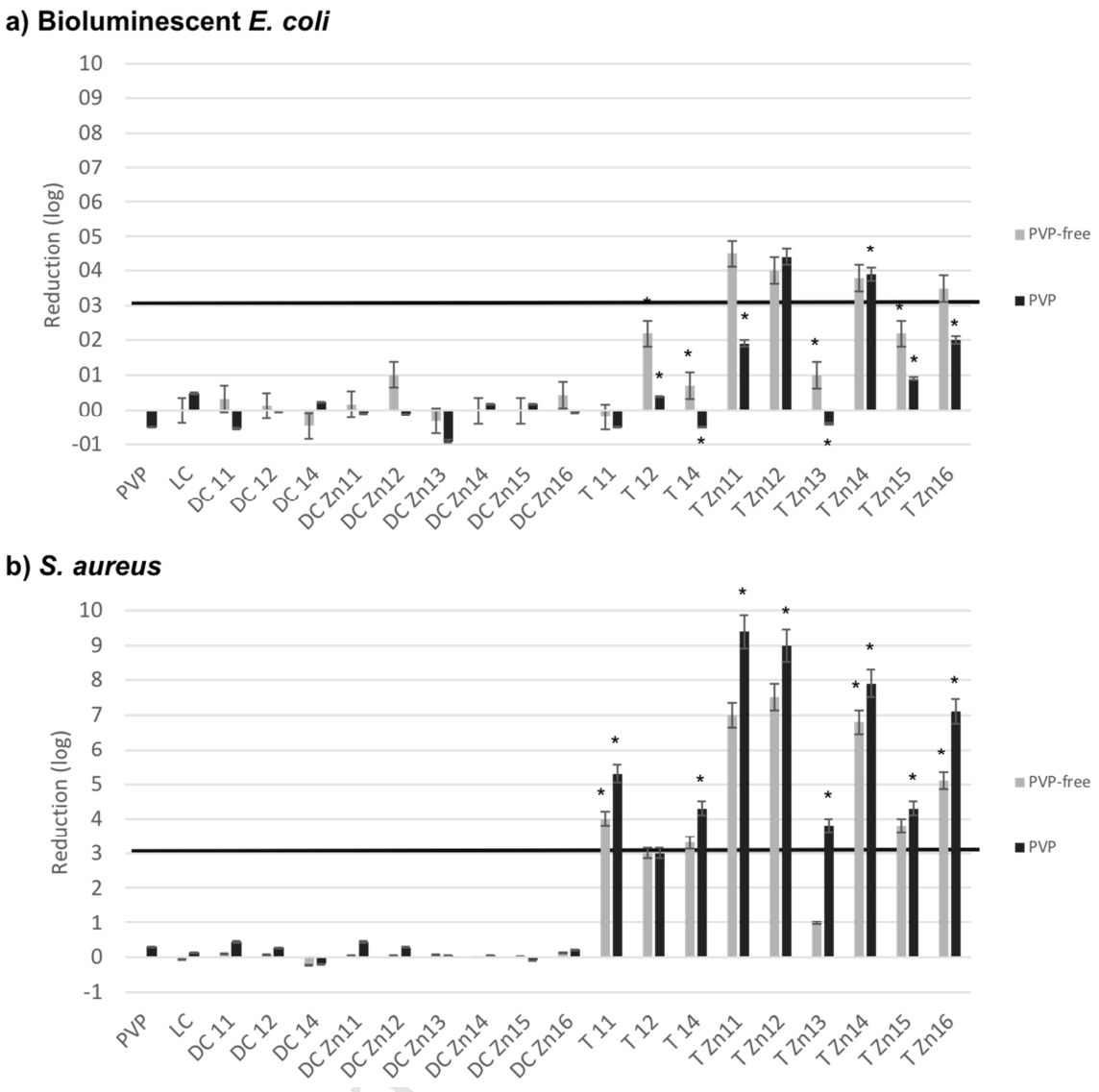

Fig. 1 Reductions (log CFU/mL) observed in the photoinactivation of Gram-negative and Gram-positive bacteria with 20 µM of each PS under red light (620–750 nm) at an irradiance of 150 mW/cm^2. a) Bioluminescent *E. coli*, after irradiation for 180 min (1620 J/cm^2) and b) *S. aureus*, after irradiation for 30 min (270 J/cm^2). Values correspond to the average of 3 independent experiments with duplicates. Error bars represent standard deviation. *Indicates a significant difference between each irradiated test and the corresponding dark control ($p < 0.05\%$). The solid line represents the 3 log threshold.

An assay with bioluminescent *E. coli* was conducted with a 20 µM PS concentration to gain a first insight on the potential of these new conjugates against Gram-negative bacteria, typically less susceptible to photosensitization [50]. The results showed that this concentration was adequate for the inactivation studies.

The results of the PDI experiments showed that the viability of the recombinant bioluminescent *E. coli* was neither affected by light alone (light control) nor by the direct effect of the PSs (dark controls). Bioluminescence without PS and without light was also stable throughout the experiments (data not shown).

PVP-free Pcs **Zn11**, **Zn12**, **Zn14** and **Zn16** were effective against bioluminescent *E. coli* with reductions equal or higher than 3 log (the ASM minimum requirement for a new antimicrobial drug) [51]. Pcs **12**, **14**, **Zn13** and **Zn15** caused a less pronounced effect and Pc **11** failed to cause a significant inactivation.

The results obtained with the encapsulated Pcs showed that only **Zn12(PVP)** and **Zn14(PVP)** caused log reductions higher than 3. All other encapsulated Pcs caused either small or non-significant inactivation *E. coli*. PVP alone (Pc unloaded control) caused a negligible effect. Significant differences were observed when comparing the results for **Zn11**/**Zn11(PVP)**, **Zn13**/**Zn13(PVP)**, and **Zn16**/**Zn16(PVP)**.

Similarly to what was observed in the experiments with bioluminescent *E. coli*, the viability of *S. aureus* was not affected by light alone (light control) nor by the direct effect of the tested PS (dark controls) but clear differences in the inactivation efficiency of the different PSs were observed. Pcs **Zn11**, **Zn12**, and **Zn14** caused the highest inactivation (>7 log reductions). Conjugates **11**, **14**, **Zn11**, **Zn12**, **Zn14**–**Zn16** caused >3 log reductions in the concentration of viable cells. As summarized in Fig. 1b, **Zn11(PVP)**–**Zn16(PVP)** were the most effective PSs causing 3.8–9.4 log inactivation.

All studied Pcs showed similar or higher efficiency in the encapsulated form when compared with the PVP-free Pcs. for *S. aureus*, the encapsulation had, in general, a positive effect on the photosensitization (Fig. 1b). As an example, **Zn13** caused *ca*. 1 log reduction while **Zn13(PVP)** caused a 3.8 log reduction (Fig. 1b). Differences between the free and encapsulated forms were statistically significant ($p < 0.05$) for **Zn11**–**Zn14** and **Zn16**.

As expected, being Gram-positive, *S. aureus* was more susceptible to photosensitization than the bioluminescent *E. coli* even for a lower light dose (270 J/cm^2 for *S. aureus* and 1620 J/cm^2 for bioluminescent *E. coli*). These results point out Pc–SA conjugates as compounds with high potential to be used as PSs of Gram-positive bacteria, and are in line with results obtained with other Pcs in the PDI of Gram-positive bacteria, including *S. aureus*, at equivalent PS concentrations [52,53].

Considering that metal-free Pcs typically cause mild photosensitization effects, and Pcs containing diamagnetic ions such as Zn and Al have higher singlet oxygen generation than those metallated with paramagnetic ions (Cu, Fe, VO) [54], the reduced inactivation effects obtained with **Pcs 11**, **12** and **14**, when compared with the good results obtained with **Zn11**, **Zn12**, **Zn14** and **Zn16**, are not a surprise. These results confirm that zinc phthalocyanines are particularly suitable for photodynamic inactivation applications due to the enhanced generation of singlet oxygen (Table 1) [3].

The tested Pc-SA conjugates have a range of *N*-substituted and *N,N*-disubstituted sulfonamide units bearing small alkyl groups (ethyl or isopropyl) or a long alkyl chain (dodecyl group) or aromatic (4-methoxyphenyl) or heteroaromatic (thiazol-2-yl) groups. The results indicate that the structure of the SA unit is an important factor for the photosensitization efficiency. The structure of the SA may influence the affinity of the PS towards important components of the cell outer structures that can ultimately determine the efficiency of binding of Pc–SA conjugates. For instance, inactivation was stronger with **Zn11** than with **Zn13**, although the % DPBF decay was smaller for **Zn11** than for **Zn13**. These results highlight that the ability to generate singlet oxygen is not the sole determinant of the photosensitization efficiency. Furthermore, two competitive pathways may be involved in the photodynamic process: the formation of radicals in biomolecules (type I mechanism) and the generation of singlet oxygen (type II mechanism). Knowing that these mechanisms may have different contributions for the inactivation outcome, even for structurally similar PSs, discussing the inactivation efficiencies of PSs based only on their ability to generate singlet oxygen may be misleading.

3. Conclusions

This work represents a new perspective in the study of Pc–SA conjugates as PSs, taking advantage of the properties of Pcs and SAs. The results discussed above demonstrate that these conjugates are promising PS for the efficient photosensitization of *E. coli* and *S. aureus,* used as Gram-negative and Gram-positive bacterial models. In addition, they confirm that the encapsulation of the Pc–SA conjugates in PVP enhances the singlet oxygen production. The results of this work clearly show that Pc–SA conjugates deserve a special attention as potential therapeutic agents against bacterial infections.

4. Experimental

4.1. Chemicals

The organic solvents used in this work were dried according to standard methods by distillation over drying agents and stored under nitrogen. All commercially available reagents were used as acquired. The progress of the reactions was monitored by thin layer chromatography (TLC), performed on silica gel-coated plastic sheets (Merck). Column chromatography was carried out using silica gel (Merck, 35–70 mesh).

4.2. Methodology

^{1}H and ^{13}C NMR spectra were acquired on Bruker DRX AC 300 or 500 instruments in $CDCl_3$ or DMSO-d_6 solutions. The frequencies used were 300.13 and 500.13 MHz for ^{1}H, and 75.47 and 125.77 MHz for ^{13}C. Chemical shifts are reported as δ values in parts per million (ppm) in relation to tetramethylsilane (TMS). Coupling constants (*J*) are in Hz. Mass spectra were obtained using an ultrafleXtreme mass spectrometer (Bruker, Bremen, Germany) controlled by Compass for flex Series 1.4, using chloroform as solvent and without matrix. The UV–Vis spectra (steady-state absorption spectra) were recorded on a UV-2501 PC spectrophotometer (Shimadzu) using glass or quartz cells of 1 cm. Steady-state emission spectra were recorded with a Fluoromax-3 spectrofluorometer (HORIBA Jobin Yvon).

4.3. Synthesis

Phthalonitriles **1**[55–57] and **4**–**6**, **9** and **10**, and phthalocyanines **Mg11**, **Mg14**, **11**, **14**, **Zn11**, **Zn14** and **Zn15** were synthesized as described in our previous works[47,48].

*4.3.1. 4-(4-Chlorosulfonylphenoxy)phthalonitrile (**2**)*

4-Phenoxyphthalonitrile **1** (1.65 g, 7.49 mmol, 1 eq.) was slowly added to chlorosulfonic acid (2.49 mL, 37.45 mmol, 5 eq.) cooled in an ice bath. The reaction

mixture was stirred for 15 minutes at a temperature between 0 °C and 5 °C and then the temperature was allowed to rise to room temperature (*ca*. 20 °C) for more 15 minutes. Thionyl chloride (1.08 mL, 14.9 mmol, 2 eq.) was added and the reaction was left for more 30 minutes at room temperature. The reaction mixture was then slowly poured onto ice (*ca*. 300 g) and the resulting solid was filtered and washed with cold water. Compound **2** was dried under vacuum at room temperature and used in the following reactions without further purification.

*4.3.2. 4-[4-(diethylaminosulfonyl)phenoxy]phthalonitrile (**3**)*

Phthalonitrile **2** (1.00 g, 3.13 mmol, 1 eq.) was dissolved in acetonitrile (5 mL) and the solution was cooled to 0 °C. Diethylamine (0.70 mL, 9.41 mmol, 3 eq.) was added slowly to the cold solution. The reaction mixture was stirred at room temperature (*ca*. 20 °C) for 2 hours and then it was poured onto ice water (*ca*. 200 g). The resulting solid was filtered off and crystallized from methanol as a white powder (0.87 g, 78% yield). ^{1}H NMR (300 MHz, $CDCl_3$): (ppm) = δ 1.18 (t, *J* = 7.1 Hz, 6H), 3.29 (q, *J* = 7.1 Hz, 4H), 7.14–7.21 (m, 2H), 7.31 (dd, *J* = 2.4, 8.7 Hz, 1H), 7.38 (d, *J* = 2.4 Hz, 1H), 7.80 (d, *J* = 8.7 Hz, 1H). ^{13}C NMR (75 MHz, $CDCl_3$) δ 160.17, 156.97, 138.09, 135.71, 129.85, 122.60, 122.41, 120.38, 118.02, 115.05, 114.66, 110.35, 42.19, 14.26. ESI-MS: 355.3 $[M]^+$.

*4.3.3. 4,5-Bis(isopropylaminosulfonylphenoxy)phthalonitrile (**7**)*

Isopropylamine (1.49 mL, 18.12 mmol, 6 eq.) was slowly added to a solution of 4,5-bis(4-chlorosulfonylphenoxy)phthalonitrile **5** (1.54 g, 3.02 mmol, 1 eq.) in acetonitrile. The mixture was stirred for 1 hour at room temperature under nitrogen atmosphere. The reaction mixture was poured into water and the resulting solid was filtered off. Recrystallization from CH_2Cl_2/hexane afforded a white powder (0.37 g, 23% yield). ^{1}H NMR (300 MHz, $CDCl_3$) δ 7.94–7.89 (m, 4H), 7.44 (s, 2H), 7.08–7.02 (m, 4H), 3.57–3.46 (m, 2H), 1.12 (d, *J* = 6.5 Hz, 12H); ^{13}C NMR (126 MHz, $CDCl_3$) δ 157.58, 150.42, 138.35, 129.73, 125.14, 118.65, 114.23, 112.77, 46.34, 23.89. ESI-MS: 555.1 $[M+H]^+$. mp: 117–123 °C.

4.3.4. 4,5-Bis(thiazol-2-ylaminosulfonylphenoxy)phthalonitrile (**8**)

To a solution of 4,5-bis(4-chlorosulfonylphenoxy)phthalonitrile (1.00 g, 1.96 mmol, 1 eq.) and 2-aminothiazole (0.196 g, 1.96 mmol, 1 eq.) in acetonitrile was slowly added triethylamine (4 eq.). The mixture was stirred for 2.5 hours under nitrogen atmosphere. The reaction was stopped with cold water and the product extracted with dichloromethane. The desired product was purified by column chromatography (silica gel) using a mixture of CH_2Cl_2/hexane (3:1) as eluent. Crystallization from CH_2Cl_2/hexane afforded the pure compound as a yellow powder (0.20 g, 16% yield). ^{1}H NMR (300 MHz, DMSO-d_6) δ 7.07 (d, *J* = 5.2 Hz, 2H), 7.33 (d, *J* = 7.9 Hz, 4H), 7.56 (dd, *J* = 1.3, 7.9 Hz, 4H), 7.75 (d, *J* = 5.2 Hz, 2H), 8.49 (s, 2H). ESI-MS: 554.6 $[M]^+$. mp: 250–253 °C.

4.3.5. Synthesis of Mg-phthalocyanines: general procedure

Magnesium turnings (9.27 mg) were added to pentan-1-ol (0.5 mL) and the suspension was heated at reflux until the complete formation of the alkoxide (overnight). Octan-1-ol (1 mL) was added to the suspension, followed by the appropriate phthalonitrile: **7** (100 mg, 0.189 mmol), **8** (100 mg, 0.157 mmol) or **3** (100 mg, 0.281 mmol). The reaction mixture was stirred overnight at 160 °C and, after cooling to room temperature (*ca*. 20 °C), it was poured onto a 5:1 methanol/water mixture (20 mL). The resulting precipitate was isolated by filtration and washed several times with methanol. Compounds **Mg12**, **Mg13** and **Mg16** were isolated as blue powders in 82%, 78% and 86% yield, respectively.

4.3.5.1. {2,3,9,10,16,17,23,24-Octakis[(4-isopropylaminosulfonyl)phenoxy]phthalocyaninato}magnesium(II) (**Mg12**)

^{1}H NMR (300 MHz, DMSO-d_6): δ 1.11 (d, *J* = 6.5 Hz, 48H), 3.44–3.55 (m, 16H), 7.02 (d, *J* = 8.8 Hz, 16H), 7.59 (d, *J* = 9.7 Hz, 8H), 7.87 (d, *J* = 8.8 Hz, 16H). MALDI: 2242.5 $[M]^+$, 2265.5 $[M+Na]^+$. mp: > 300 °C.

4.3.5.2. {2,3,9,10,16,17,23,24-Octakis[(4-thiazol-2-ylaminosulfonyl)phenoxy]phthalocyaninato}magnesium(II) (**Mg13**)

^{1}H NMR (500 MHz, $CDCl_3$): δ 6.89–7.11 (m, 24H), 7.33–7.55 (m, 16H), 7.56–7.86 m, 16H). MALDI: 1277.9 $[M+2H]^{2+}$. mp: > 300 °C.

*4.3.5.3. {2,9(10),16(17),23(24)-Tetrakis[(4-(diethylaminosulfonyl)phenoxy]phthalocyaninato}magnesium(II) (**Mg16**)*

^{1}H NMR (500 MHz, $CDCl_3$): δ 1.13–1.19 (m, 24H), 3.21–3.30 (m, 16H), 7.11–7.20 (m, 4H), 7.45–7.98 (m, 24H). MALDI: 1444.4 $[M]^+$. mp: > 300 °C.

4.3.6. Synthesis of Zn-phthalocyanines: general procedure

The magnesium phthalocyanine (**Mg12**, **Mg13** or **Mg16**) was dissolved in dry THF (20 mL) in a 50 mL flask equipped with a water condenser. Trifluoroacetic acid (2 mL) was added and the mixture was heated at 50 °C for 3 hours. The removal of the coordinated Mg^{2+} was monitored by UV–Vis spectroscopy and TLC. The reaction mixture was cooled to room temperature (*ca*. 20 °C) and water (*ca*. 10 mL) was added until a precipitate was formed. Methanol (2 mL) was also added leading to additional precipitation. The metal-free phthalocyanine was then collected by filtration. The solid was dissolved in a minimal amount of DMF, zinc acetate (2.5 eq.) was added and the mixture was left overnight at 150 °C in a sealed tube. The metallation was confirmed by UV–Vis analysis. The reaction mixture was cooled to room temperature and water (*ca*. 10 mL) was added until a precipitate was formed. Methanol (2 mL) was added and the product was collected by filtration. The solid was dissolved in dichloromethane and the solution was dried with anhydrous sodium sulfate. The zinc phthalocyanine (**Zn12**, **Zn13** or **Zn16**) was crystalized form dichloromethane/hexane and the crystals were dried under vacuum.

4.4. Encapsulation of phthalocyanines in polyvinylpyrrolidone (PVP)

From 1 mM stock solutions of phthalocyanines **11**, **12**, **14** and **Zn11**–**Zn16** in dichloromethane, 0.5 mL were placed in sample ports with 100 mg of PVP (40 kDa). As a control, one of the sample ports was prepared in the same way but containing only PVP and dichloromethane (0.5 mL). The resulting solutions were evaporated with N_2 until oil formation. The sample ports were left at 55 °C overnight. The resulting polymers were suspended in distilled water (1 mL) and solubilized under ultrasounds (Bandelin Sonorex Digitec DT 255 H, 50/60 Hz, Germany) for approximately 10 minutes.

4.5. Photosensitizer stock solutions

Stock solutions of the conjugates used in solubility and photostability tests, singlet oxygen generation and photodynamic inactivation assays were prepared in dimethyl sulfoxide (DMSO) for PVP-free conjugates and in distilled water for PVP encapsulated conjugates at a concentration of 500 μM and diluted in DMF/H_2O (9:1) or phosphate buffered saline (PBS), depending of the experiments, to obtain the working concentration.

4.6. Phthalocyanine solubility tests

The solubility of the phthalocyanine–sulfonamide conjugates **11**, **12**, **14** and **Zn11**–**Zn16**, and the corresponding Pc–SA conjugates encapsulated in PVP, in DMSO and PBS was assessed by UV–Vis spectroscopy. Concentrations between 0.625 μmol/L and 25 μmol/L, obtained by the addition of aliquots of each Pc 500 mM stock solution, were analysed. The intensity of the Q-band versus Pc concentration was plotted in a graphic for linear regression to determine the concentrations that follow the Beer–Lambert law.

4.7. Photostability tests

The photobleaching rates of compounds **11**, **12**, **14** and **Zn11**–**Zn16,** and the corresponding Pc–SA conjugates encapsulated in PVP, were determined by irradiating 2 mL of a diluted solution of each Pc in PBS under the conditions used in the biological assays (red light at 150 mW/cm^2). During irradiation, the solutions were magnetically stirred and kept at room temperature (*ca.* 20 °C). The concentration of the Pc derivative was quantified at regular time intervals by UV–Vis spectroscopy. The intensity of the Q-band at different time intervals and the photostability was expressed as I_t/I_0 (%; I_t = intensity of the band at given time of irradiation, I_0 = intensity of the band before irradiation). Similar stability tests were performed in the dark to account for the effect of aggregation as a source of light-independent decay. The conjugates were considered photostable when the difference between the value of I_t/I_0 of the photostability tests and the value of I_t/I_0 of the stability tests were no higher than 5%.

4.8. Singlet oxygen generation

The ability of each Pc and Pc(PVP) to generate singlet oxygen was qualitatively evaluated following the photo-oxidation of 1,3-diphenylisobenzofuran (DPBF), a singlet oxygen quencher [58]. Stock solutions of each PS at 0.5 mmol/L in DMF and a stock solution of DPBF at 50 mmol/L in DMF/H_2O (9:1) were prepared. Mixtures of each phthalocyanine derivative and DPBF were irradiated with a LED array composed of 25 light sources with an emission peak at 640 nm and a bandwidth at half maximum of ± 20 nm, at an irradiance of 9.0 mW/cm^2. The absorption decay of DPBF at 415 nm was measured at irradiation intervals of 1 min, during 7 min. The DPBF absorption decay, that is proportional to the production of $^1O_2$, was assessed by the quotient between the absorbance of DPBF at a given irradiation time and the initial absorbance.

4.9. Bacterial strains, growth conditions and preparation of stock-suspensions

A recombinant bioluminescent strain of *Escherichia coli*, transformed with plasmids pHK724 and pHK555 containing the lux operon from the bioluminescent marine bacterium *Vibrio fischeri* [59] was used as a model for Gram-negative bacteria [60]. Before each PDI assay, one isolated colony from a culture growing on Tryptic Soy Agar (TSA, Merck) amended with the antibiotics ampicillin (100 mg/mL) and chloramphenicol (25 mg/mL) was aseptically inoculated on Tryptic Soy Broth (TSB, Merck) with both antibiotics and grown overnight at 26 °C under stirring (130 rpm) at aerobic atmosphere. An aliquot of this primary culture was sub-cultured in TSB with the same antibiotics and growth overnight under the same conditions (130 rpm, 26 °C and at aerobic atmosphere), and used to prepare the cell suspensions for the PDI assays.

To confirm the correlation between the bioluminescent signal (in relative light units, RLU) of *E. coli* and the concentration of colony forming units (CFU), two independent assays were carried out. An overnight culture (~10^7 CFU/mL) of bioluminescent *E. coli* was serially diluted (10^1 to 10^7) in PBS. Light emission of the non-diluted and diluted aliquots was read on a luminometer (Turner Designs – 20/20). Viable counts were determined by pour-plating two replicates of each dilution in TSA medium. After 24 h of incubation at 37 °C (aerobic atmosphere), colonies were counted in the most convenient dilution series. Three independent assays were conducted.

Staphylococcus aureus (ATCC 29213) was used as a model for Gram-positive bacteria [61,62]. Stock cultures in TSA were kept at 4 °C. Fresh cultures were prepared before each assay by inoculating an isolated colony in 30 mL of TSB. The cultures were incubated for 24 h at 37 °C under stirring (130 rpm) and at aerobic atmosphere. An aliquot of this primary culture was sub-cultured in TSB, grown overnight under stirring (130 rpm) at 37 °C and at aerobic atmosphere to obtain fresh cultures for the PDI assays.

4.10. Photodynamic inactivation assays

For the PDI assays, fresh liquid cultures of each bacterium were 10-fold diluted in PBS and allowed to stabilize under stirring for 10 minutes, at room temperature (*ca*. 20 °C). Aliquots of 0.1 mL were distributed into 1 mL vials and added of 0.04 mL stock-solution of the Pc (sonicated for 30 minutes before used) (4% final concentration of DMSO), or aqueous suspensions of Pc(PVP), to achieve final concentrations of 20 μM of Pc. The experiments were conducted in 3 independent assays with duplicates. After adding the PS, the suspensions were pre-incubated in the dark, at 37 °C (aerobic atmosphere), for 30 min for adsorption of the PS to the cells and then were irradiated with red light. The light source was an illumination system (LC-122 LumaCare, London) equipped with a 250 W quartz halogen (mixed) lamp, coupled to an interchangeable fiber optic probe at 620–750 nm [63]. Lamp maximum spectral irradiance wavelength is observed between 550 and 650 nm. The irradiance was set to 150 mW/cm^2 and confirmed with an energy meter Coherent FieldMaxII-Top combined with a Coherent PowerSensPS19Q energy sensor. Irradiation area covered 3 samples (1 test sample, 1 light control and 1 dark control – the latter was covered with aluminium foil). The irradiance was equal in all 3 samples. Irradiance at the sample level was set to 150 mW/cm^2 by adjusting the distance of the optical fiber probe to the sample. The inactivation of bacteria was evaluated upon irradiation with red light for 0 (0), 10 (90), 20 (180), 30 (270), 60 (540), 90 (810), 120 (1080), 180 (1620) min (J/cm^2) for bioluminescent *E. coli*, and for 0 (0), 10 (90), 20 (180) and 30 (270) min (J/cm^2) for *S. aureus*, at a PS concentration of 20 μM. Aliquots were periodically collected for measurement of bioluminescence, in the case of *E. coli*, or for the determination of the concentration of viable cells by colony counting, in the case of *S. aureus*. Bioluminescence was measured in triplicate aliquots with a luminometer (TD-20⁄20 Luminometer; Turner Designs, Inc.). To determine the concentration of viable cells, the suspension of *S. aureus* was serially diluted

in PBS and triplicates of the convenient dilutions were pour-plated in TSA. These cultures were incubated at 37 °C for 24 h. Colonies were counted in the replicates of the most suitable dilution and the concentration of viable cells was expressed as CFU/mL. Light (without PS) and dark (protected from light) controls were included in all experiments.

4.11. Statistical analysis

Statistical analysis was performed with SPSS package (IBM SPSS analytics 24.0). Normal distribution was verified by the Kolmogorov–Smirnov test. The significance of irradiation time and type of PS on bacterial inactivation between light and dark controls and the test groups in which the bacteria were irradiated with the proper light in the presence of the PS, between test groups for the different light conditions and between the same conjugate encapsulated with PVP or not, was assessed by non-parametric univariate analysis of variance (non-parametric ANOVA) model with the Viruskal–Wallis test. A value of $p < 0.05$ was considered significant.

Acknowledgements

Thanks are due to University of Aveiro and FCT/MEC for the financial support to the QOPNA research project (FCT UID/QUI/00062/2013) and the CESAM Research Unit (PEst-C/MAR/LA0017/2013) through national funds, and where applicable co-financed by the FEDER, within the PT2020 Partnership Agreement, and also to the Portuguese NMR Network. R. N. Silva thanks FCT for her PhD grant (SFRH/BD/87598/2012). We also thank Doctor Ana Gomes, from the Department of Chemistry, University of Aveiro, for the assistance in the experiments with PVP.

References

[1] C.G. Claessens, U. Hahn, T. Torres, Phthalocyanines: From outstanding electronic properties to emerging applications, Chem. Rec. 8 (2008) 75–97.

[2] Y. Bian, J. Jiang, Recent Advances in Phthalocyanine-based functional molecular materials, Struct. Bond. 172 (2015) 159–199.

[3] E. Ben-Hur, W.S. Chan, Phthalocyanines in photobiology and their medical applications, in: K. Kadish, K.M. Smith, R. Guilard (Eds.), The Porphyrin Handbook:

Applications of Phthalocyanines, Vol. 19, pp. 1–35, Academic Press, San Diego, 2003.

[4] A.R.M. Soares, M.G.P.M.S. Neves, A.C. Tomé, M.C. Iglesias-de La Cruz, A. Zamarrón, E. Carrasco, S. González, J. Cavaleiro, T. Torres, D.M. Guldi, A. Juarranz, Glycophthalocyanines as photosensitizers for triggering mitotic catastrophe and apoptosis in cancer cells, Chem. Res. Toxicol. 25 (2012) 940–951.

[5] S.G. Kimani, T.A. Shmigol, S. Hammond, J.B. Phillips, J.I. Bruce, A.J. MacRobert, M. V. Malakhov, J.P. Golding, Fully protected glycosylated zinc (II) phthalocyanine shows high uptake and photodynamic cytotoxicity in MCF-7 cancer cells, Photochem. Photobiol. 89 (2013) 139–149.

[6] L.M.O. Lourenço, P.M.R. Pereira, E. Maciel, M. Válega, F.M.J. Domingues, M.R.M. Domingues, M.G.P.M.S. Neves, J.A.S. Cavaleiro, R. Fernandes, J.P.C. Tomé, Amphiphilic phthalocyanine-cyclodextrin conjugates for cancer photodynamic therapy., Chem. Commun. 50 (2014) 8363–8366.

[7] L.M.O. Lourenço, A. Sousa, M.C. Gomes, M.A.F. Faustino, A. Almeida, A.M.S. Silva, M.G.P.M.S. Neves, J.A.S. Cavaleiro, Â. Cunha, J.P.C. Tomé, Inverted methoxypyridinium phthalocyanines for PDI of pathogenic bacteria, Photochem. Photobiol. Sci. 14 (2015) 1853–1863.

[8] D.M. Rocha, N. Venkatramaiah, M.C. Gomes, A. Almeida, M.A.F. Faustino, F.A. Almeida Paz, Â. Cunha, J.P.C. Tomé, Photodynamic inactivation of Escherichia coli with cationic ammonium Zn(II) phthalocyanines, Photochem. Photobiol. Sci. 14 (2015) 1872–1879.

[9] J.F. Lovell, P.-C. Lo, Porphyrins and phthalocyanines for theranostics, Theranostics 2 (2012) 815–816.

[10] Y. Zhang, J.F. Lovell, Recent applications of phthalocyanines and naphthalocyanines for imaging and therapy, Wiley Interdiscip. Rev. Nanomedicine Nanobiotechnology 9 (2017) e1420.

[11] B. Brozek-Pluska, M. Orlikowski, H. Abramczyk, Phthalocyanines: From dyes to photosensitizers in diagnostics and treatment of cancer. Spectroscopy and Raman imaging studies of phthalocyanines in human breast tissues, in: K. Kadish, K.M. Smith, R. Guilard (Eds.), Handbook of Porphyrin Science, Vol. 39, pp. 1–49, 2016.

[12] A.A. Valiente-Gabioud, M.C. Miotto, M.E. Chesta, V. Lombardo, A. Binolfi, C.O. Fernández, Phthalocyanines as molecular scaffolds to block disease-associated

protein aggregation, Acc. Chem. Res. 49 (2016) 801–808.

[13] M. Bouvet, P. Gaudillat, J.-M. Suisse, Phthalocyanine-based hybrid materials for chemosensing, J. Porphyr. Phthalocyanines 17 (2013) 913–919.

[14] W.C. Trogler, Chemical sensing with semiconducting metal phthalocyanines, Struct. Bond. 142 (2012) 91–118.

[15] J. Ahmed, Y. Yuan, L. Zhou, S. Kim, Carbon supported cobalt oxide nanoparticles-iron phthalocyanine as alternative cathode catalyst for oxygen reduction in microbial fuel cells, J. Power Sources 208 (2012) 170–175.

[16] Y. Yuan, J. Ahmed, S. Kim, Polyaniline/carbon black composite-supported iron phthalocyanine as an oxygen reduction catalyst for microbial fuel cells, J. Power Sources 196 (2011) 1103–1106.

[17] B. Turanli-Yildiz, T. Sezgin, Z.P. Akar, C. Uslan, B.Ş. Sesalan, A. Gül, The use of novel photobleachable phthalocyanines to image DNA, Synth. Met. 161 (2011) 1720–1724.

[18] C. Uslan, B. Şebnem Sesalan, Synthesis of novel DNA-interacting phthalocyanines, Dyes Pigments 94 (2012) 127–135.

[19] A.B. Sorokin, Phthalocyanine metal complexes in catalysis, Chem. Rev. 113 (2013) 8152–8191.

[20] M.E. Ragoussi, M. Ince, T. Torres, Recent advances in phthalocyanine-based sensitizers for dye-sensitized solar cells, Eur. J. Org. Chem. (2013) 6475–6489.

[21] M.E. Ragoussi, T. Torres, Modern synthetic tools toward the preparation of sophisticated phthalocyanine-based photoactive systems, Chem. Asian J. 9 (2014) 2676–2707.

[22] R. Karaman, Commonly used drugs - Uses, side effects, bioavailability and approaches to improve it, Nova Science Pub Inc, Hauppauge, New York, 2015.

[23] P. Klahn, M. Brönstrup, New structural templates for clinically validated and novel targets in antimicrobial drug research and development, Curr. Top. Microbiol. Immunol. 398 (2016) 365–417.

[24] A. Bermingham, J.P. Derrick, The folic acid biosynthesis pathway in bacteria: Evaluation of potential for antibacterial drug discovery, BioEssays 24 (2002) 637–648.

[25] S. Bag, R. Tulsan, A. Sood, H. Cho, H. Redjeb, W. Zhou, H. Levine, B. Török, M. Török, Sulfonamides as multifunctional agents for Alzheimer's disease, Bioorg. Med. Chem. Lett. 25 (2015) 626–630.

[26] Z. Chen, Z.-C. Wang, X.-Q. Yan, P.-F. Wang, X.-Y. Lu, L.-W. Chen, H.-L. Zhu, H.-W. Zhang, Design, synthesis, biological evaluation and molecular modeling of dihydropyrazole sulfonamide derivatives as potential COX-1/COX-2 inhibitors, Bioorg. Med. Chem. Lett. 25 (2015) 1947–1951.

[27] F.A. Abulwerdi, C. Liao, A.S. Mady, J. Gavin, C. Shen, T. Cierpicki, J.A. Stuckey, H.D.H. Showalter, Z. Nikolovska-Coleska, 3-substituted-N-(4-hydroxynaphthalen-1-yl)arylsulfonamides as a novel class of selective Mcl-1 inhibitors: Structure-based design, synthesis, SAR, and biological evaluation, J. Med. Chem. 57 (2014) 4111–4133.

[28] M. Kołaczkowski, M. Marcinkowska, A. Bucki, M. Pawłowski, K. Mitka, J. Jaśkowska, P. Kowalski, G. Kazek, A. Siwek, A. Wasik, A. Wesołowska, P. Mierzejewski, P. Bienkowski, Novel arylsulfonamide derivatives with 5-HT6/5-HT7 receptor antagonism targeting behavioral and psychological symptoms of dementia, J. Med. Chem. 57 (2014) 4543–4557.

[29] G. De Simone, A. Di Fiore, C. Capasso, C.T. Supuran, The zinc coordination pattern in the η-carbonic anhydrase from Plasmodium falciparum is different from all other carbonic anhydrase genetic families, Bioorg. Med. Chem. Lett. 25 (2015) 1385–1389.

[30] L. Syrjänen, M. Kuuslahti, M. Tolvanen, D. Vullo, S. Parkkila, C.T. Supuran, The β-carbonic anhydrase from the malaria mosquito Anopheles gambiae is highly inhibited by sulfonamides, Bioorg. Med. Chem. 23 (2015) 2303–2309.

[31] S.P. Sahoo, B.B. Subudhi, Development of amino acid conjugated sulfonamides as potent antiulcer agent, Med. Chem. Res. 23 (2014) 3039–3048.

[32] M.R. Ke, S.F. Chen, X.H. Peng, Q.F. Zheng, B.Y. Zheng, C.K. Yeh, J.D. Huang, A tumor-targeted activatable phthalocyanine-tetrapeptide-doxorubicin conjugate for synergistic chemo-photodynamic therapy, Eur. J. Med. Chem. 127 (2017) 200–209.

[33] P. Tomanová, S. Rimpelová, M. Jurášek, M. Buděšínský, L. Vejvodová, T. Ruml, E. Kmoníčková, P.B. Drašar, Trilobolide-porphyrin conjugates: On synthesis and biological effects evaluation, Steroids 97 (2015) 8–12.

[34] X. Zheng, Z. Li, L. Chen, Z. Xie, X. Jing, Self-assembly of porphyrin–paclitaxel conjugates into nanomedicines: enhanced cytotoxicity due to endosomal escape, Chem. Asian J. 11 (2016) 1780–1784.

[35] S. Padilla-Monroy, E. Martínez-Klimova, T. Ramírez-Ápan, A. Nieto-Camacho, J. Calderón-Pardo, M. Martínez-García, Porphyrin conjugates of Ibuprofen and their

antiproliferative activity against human prostate and breast cancer cells, Biointerface Res. Appl. Chem. 8 (2018) 3039–3047.

[36] H.S. Jung, J. Han, H. Shi, S. Koo, H. Singh, H.J. Kim, J.L. Sessler, J.Y. Lee, J.H. Kim, J.S. Kim, Overcoming the limits of hypoxia in photodynamic therapy: A carbonic anhydrase IX-targeted approach, J. Am. Chem. Soc. 139 (2017) 7595–7602.

[37] T. Zhang, W. Zhang, M. Zheng, Z. Xie, Near-infrared BODIPY-paclitaxel conjugates assembling organic nanoparticles for chemotherapy and bioimaging, J. Colloid Interface Sci. 514 (2018) 584–591.

[38] Y. Li, X. Hu, X. Zheng, Y. Liu, S. Liu, Y. Yue, Z. Xie, Self-assembled organic nanorods for dual chemo-photodynamic therapies, RSC Adv. 8 (2018) 5493–5499.

[39] A.W. Snow, Phthalocyanine Aggregation, in: K. Kadish, K.M. Smith, R. Guilard (Eds.), The Porphyrin Handbook - Phthalocyanines: Properties and Materials, Vol. 17, pp. 129-176, Academic Press, San Diego, 2003.

[40] B.Y. Zheng, M.R. Ke, W.L. Lan, L. Hou, J. Guo, D.H. Wan, L.Z. Cheong, J.D. Huang, Mono- and tetra-substituted zinc(II) phthalocyanines containing morpholinyl moieties: Synthesis, antifungal photodynamic activities, and structure-activity relationships, Eur. J. Med. Chem. 114 (2016) 380–389.

[41] B. Pucelik, I. Gürol, V. Ahsen, F. Dumoulin, J.M. Dąbrowski, Fluorination of phthalocyanine substituents: Improved photoproperties and enhanced photodynamic efficacy after optimal micellar formulations, Eur. J. Med. Chem. 124 (2016) 284–298.

[42] M. Hädener, I. Gjuroski, J. Furrer, M. Vermathen, Interactions of polyvinylpyrrolidone with chlorin e6-based photosensitizers studied by NMR and electronic absorption spectroscopy, J. Phys. Chem. B 119 (2015) 12117–12128.

[43] R. Liang, L. Ma, L. Zhang, C. Li, W. Liu, M. Wei, D. Yan, D.G. Evans, X. Duan, A monomeric photosensitizer for targeted cancer therapy, Chem. Commun. 50 (2014) 14983–14986.

[44] M. V. Parkhats, V.A. Galievsky, A.S. Stashevsky, T. V. Trukhacheva, B.M. Dzhagarov, Dynamics and efficiency of the photosensitized singlet oxygen formation by chlorin e 6: The effects of the solution pH and polyvinylpyrrolidone, Opt. Spectrosc. 107 (2009) 974–980.

[45] A.G. Bobylev, Y. V. Shatalin, I.M. Vikhlyantsev, L.G. Bobyleva, S. V. Gudkov, Z.A. Podlubnaya, Interaction of C60 fullerene-polyvinylpyrrolidone complex and brain

Aβ(1–42)-peptide in vitro, Biophysics 59 (2014) 685–688.

[46] E. Fagadar-Cosma, E. Tarabukina, N. Zakharova, M. Birdeanu, B. Taranu, A. Palade, I. Creanga, A. Lascu, G. Fagadar-Cosma, Hybrids formed between polyvinylpyrrolidone and an A3B porphyrin dye: Behaviour in aqueous solutions and chemical response to CO2 presence, Polym. Int. 65 (2016) 200–209.

[47] E.F.A. Carvalho, M.J.F. Calvete, A.C. Tomé, J.A.S. Cavaleiro, Synthesis of sulfonamide-substituted phthalocyanines, Tetrahedron Lett. 50 (2009) 6882–6885.

[48] E.F.A. Carvalho, M.J.F. Calvete, J.A.S. Cavaleiro, D. Dini, M. Meneghetti, A.C. Tomé, Synthesis and high ranked NLT properties of new sulfonamide-substituted indium phthalocyanines, Inorganica Chim. Acta 363 (2010) 3945–3950.

[49] M. Price, J.J. Reiners, A.M. Santiago, D. Kessel, Monitoring singlet oxygen and hydroxyl radical formation with fluorescent probes during photodynamic therapy, Photochem. Photobiol. 85 (2009) 1177–1181.

[50] E. Alves, L. Costa, C.M. Carvalho, J.P. Tomé, M.A. Faustino, M.G. Neves, A.C. Tomé, J.A. Cavaleiro, A. Cunha, A. Almeida, Charge effect on the photoinactivation of gram-negative and gram-positive bacteria by cationic meso-substituted porphyrins, BMC Microbiol. 9 (2009) 70.

[51] F. Cieplik, L. Tabenski, W. Buchalla, T. Maisch, Antimicrobial photodynamic therapy for inactivation of biofilms formed by oral key pathogens, Front. Microbiol. 12 (2014) 405.

[52] G.C. Taşkin, M. Durmuş, F. Yüksel, V. Mantareva, V. Kussovski, I. Angelov, D. Atilla, Axially paraben substituted silicon(IV) phthalocyanines towards dental pathogen Streptococcus mutans: Synthesis, photophysical, photochemical and in vitro properties, J. Photochem. Photobiol. A 306 (2015) 31–40.

[53] N. Masilela, E. Antunes, T. Nyokong, Axial coordination of zinc and silicon phthalocyanines to silver and gold nanoparticles: an investigation of their photophysicochemical and antimicrobial behavior, J. Porphyr. Phthalocyanines 17 (2013) 417–430.

[54] C.C. Leznoff, A.B.P. Lever, Phthalocyanines: properties and applications, VCH Publishers, New York, 1989.

[55] N.E. Galanin, E. V. Kudrik, G.P. Shaposhnikov, 4-Tetraphenyl-and 4-tetraphenoxy-substituted meso-tetraphenyltetrabenzoporphyrins. Synthesis and spectral

properties, Russ. J. Org. Chem. 42 (2006) 603–606.

[56] P. Tau, T. Nyokong, Synthesis and electrochemical characterisation of α- and β-tetra-substituted oxo(phthalocyaninato) titanium(IV) complexes, Polyhedron 25 (2006) 1802–1810.

[57] X.-F.F. Zhang, Y. Wang, L. Niu, Titanyl phthalocyanine and its soluble derivatives: Highly efficient photosensitizers for singlet oxygen production, J. Photochem. Photobiol. A 209 (2010) 232–237.

[58] C. Barner-Kowollik, A.J. Inglis, Has click chemistry lead to a paradigm shift in polymer material design?, Macromol. Chem. Phys. 210 (2009) 987–992.

[59] E. Alves, C.M.B. Carvalho, J.P.C. Tomé, M.A.F. Faustino, M.G.P.M.S. Neves, A.C. Tomé, J.A.S. Cavaleiro, Â. Cunha, S. Mendo, A. Almeida, Photodynamic inactivation of recombinant bioluminescent Escherichia coli by cationic porphyrins under artificial and solar irradiation, J. Ind. Microbiol. Biotechnol. 35 (2008) 1447–1454.

[60] E. Alves, L. Costa, Â. Cunha, M.A.F. Faustino, M.G.P.M.S. Neves, A. Almeida, Bioluminescence and its application in the monitoring of antimicrobial photodynamic therapy, Appl. Microbiol. Biotechnol. 92 (2011) 1115–1128.

[61] N. Tortik, A. Spaeth, K. Plaetzer, Photodynamic decontamination of foodstuff from Staphylococcus aureus based on novel formulations of curcumin, Photochem. Photobiol. Sci. 13 (2014) 1402–1409.

[62] Y. Arenas, S. Monro, G. Shi, A. Mandel, S. McFarland, L. Lilge, Photodynamic inactivation of Staphylococcus aureus and methicillin-resistant Staphylococcus aureus with Ru(II)-based type I/type II photosensitizers, Photodiagnosis Photodyn. Ther. 10 (2013) 615–625.

[63] L. Costa, C.M.B. Carvalho, M.A.F. Faustino, M.G.P.M.S. Neves, J.P.C. Tomé, A.C. Tomé, J.A.S. Cavaleiro, Â. Cunha, A. Almeida, Sewage bacteriophage inactivation by cationic porphyrins: influence of light parameters, Photochem. Photobiol. Sci. 9 (2010) 1126–1133.

Highlights

- Synthesis of phthalocyanines bearing four or eight sulfonamide units
- Phthalocyanine–sulfonamide conjugates encapsulated within PVP micelles
- Photodynamic inactivation of Gram-negative and Gram-positive bacteria